Design of a Boxlift Crane

MAE 321 Midterm Design Project

October 25, 2013

Designed by: Gabriel Baraban, David Beck, Annie Cardinal, Richard Cheng, Adam Fisch, Sebastian Grimberg and Po Wah Moon

Table of Contents

Executive Summary

Fabricating a boxlift crane involves many challenges that must be considered in order to be successful. Similar to the design of aircraft wings, a boxlift crane is a lightweight, cantilevered, semi-monocoque structure. Semi-monocoque structures such as the crane are designed such that the external metal skin absorbs all or most of the stresses to which the body is subjected. The internal frame and support system also helps to bear a portion of the load, distributes stress throughout the structure, and provides rigidity.

Our project team was presented with the task of manufacturing a crane that can support 500 pounds both in symmetric and asymmetric loading. The weight would be suspended at a pin a minimum of 28 inches away from a support column, to which the crane is connected via two pins. In addition to withstanding failure, the boxlift crane also had to meet several strict design specifications:

- The weight shall not exceed 3 pounds.
- The beam can hold 500 pounds on the ½ chord and ¼ chord, at a distance greater than .85L from the root.
- The max vertical deflection allowed at the tip is 4 inches.
- The root section must be 6 inches in chord and less than 5 inches in thickness.
- The thickness at the free end (tip) of the box must be less than 3 inches.
- The beam must have a planform taper ratio between 0.5 and 0.75.
- The beam aspect ratio, L^2/S, must exceed 6.5.
- The distance from the pin holding the load to the base of the column must exceed 28 inches.
- The magnitude of a dihedral angle, if present, should not exceed 10°.
- Materials must be aluminum alloys.

The philosophy behind our final design decisions consisted of a desire for simplicity, elegance, and strength. A key objective was to maximize the ratio of strength to weight. Therefore, comprehensive analysis was done to reduce the crane to only its essential components.

In addition, the crane's length and taper ratio were optimized to resist both bending and torsion. This optimization took into account the effects of the crane dimensions on critical geometrical properties such as the moment of inertia (I) and the polar moment of inertia (J). Our design had an overall length of 30 in, a planform taper ratio of 0.53, and an aspect ratio of 6.52. The skin is made of 1/32'' thick 2024 aluminum, which was selected over other alloys for its superior strength and stiffness. Simple circular cuts in the skins significantly reduce the weight while ensuring ease of manufacturing and completion with time to spare. Lightweight ribs strategically placed in the crane greatly increase resistance to torsion, while adding minimal weight to the structure. Fully assembled, the crane weighs merely 2 pounds 10 ounces — slightly over 85% of the weight limit.

Using 3D modeling and FEM in the Creo Parametric software package, the boxlift crane was tested and optimized to its dimensions stated above. The final design iteration exhibited a crane design that performed exceptionally well in all of the computational bending, torsion, and buckling studies. Static analyses and failure index tests show that the maximum stresses in the structure are well below the yield limit of 2024 aluminum. Based on our simulations in Creo and rivet calculations, we expect the crane to be able to support 760 lbs before failure.

The design of light and strong structures is increasingly valuable in the modern world where extra weight often carries a harsh energy consumption cost and resource penalty. On a larger scale with slight modifications, our semi-monocoque structure would be marketable and adaptable to various structural uses such as aircraft, automobiles, and other frameworks.

I. Introduction

Our project team was presented with the challenge of building a boxlift crane capable of supporting significant weight. Our objective was to meet the design demands and manufacture a lightweight yet strong structure. Our crane also had to be more than just functional; in accord with proper engineering production guidelines, the crane should be safe, reliable, easy to manufacture, and marketable as well. Thus additional motivations in the design process were that the crane should be strong enough to withstand even greater than the goal load, that it should be aesthetic, and not overly complex to machine.

The specifications and constraints set forth in the problem statement were extensive. The crane should be a hollow beam of length L and minimal weight that met the requirements below:

DESIGN SPECIFICATIONS:

1. The structural weight of the assembled beam shall not exceed 3 pounds.
2. The beam should be capable of lifting and holding at least 500 pounds on the mid chord line as well as on the quarter chord line, at a distance greater than .85L from the root.
3. When loaded, the maximum vertical deflection allowed at the tip is 4 inches.
4. The root section must be 6 inches in chord, less than 5 inches in thickness, and must be secured to the test-bed column via two pins.
5. The thickness at the free end (tip) of the box must be less than 3 inches.
6. The beam must be tapered in planform, with a taper ratio of
$$\lambda = .5 \leq \frac{ctip}{croot} \leq .75$$
7. The beam aspect ratio, equal to L^2/S, must exceed 6.5. S is the planform area (top view) and L is the length of the beam.
8. The distance from the pin holding the load to the base of the column must exceed 28 inches.
9. The magnitude of a dihedral angle, if present, should not exceed 10°.
10. The structure must be fabricated from aluminum alloys.

The basic concepts behind our design come from solid mechanics. The principal stresses imposed on the beam due to the loading are shear stresses, bending moments, and torsion.

When the load is applied at the mid chord line, the main stress will be a large bending moment. When fixed to the test-bed column, the crane functions as a cantilevered beam. In that support system, the moment increases linearly from a minimum at the tip to a maximum at the root. The bending moment produces a tension in the top surface and compression in the bottom surface, with the stress varying over the beam cross-section according to [5]:

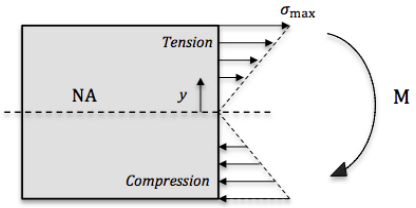

Figure 1: Stress due to bending

$$Local\ stress = \sigma = \frac{My}{I} \quad (1)$$

Where M is the bending moment at the section, I is the moment of inertia of the cross section about the neutral axis, and y is the distance from the neutral axis. Maximizing the moment of inertia of the cross section was an important step in minimizing stresses on the beam.

Another mode of failure introduced by the loading is buckling. Since the crane must be hollow, the bottom plate bears nearly all of the compressive force. Buckling is not so much of a failure of the material, but rather characterized by a mathematical, geometrical, elastic instability. In long slender beams, high compression forces can cause a beam to bow outwards — and fail shortly thereafter. The critical load for buckling is given by the Euler Buckling Formula [5]:

$$P_{critical} = \frac{P^2 EI}{(L_e)^2} \quad (2)$$

P is the axial compressive force, E is the Young's Modulus, I is the cross sectional moment of inertia, and L_e is the effective length of the member. To counteract buckling, the bottom plate can either be stiffened by increasing I, or braced widthwise such so that the effective length is reduced.

Alternatively, when the load is applied at the quarter chord line, the main stress will be torsional due to the large torque applied to the beam cross section. The torque causes a linear variation the shear stress along any cross-sectional radial line [5].

$$Local\ shear\ stress \quad = \quad \tau \quad = \quad \frac{T\rho}{J} \tag{3}$$

T is the internal torque acting at the cross section, ρ is the radial distance from the centroid, and J is the polar moment of inertia. As for the bending stress, in order to resist the torsional stress, it is important to maximize the polar moment of inertia of the beam.

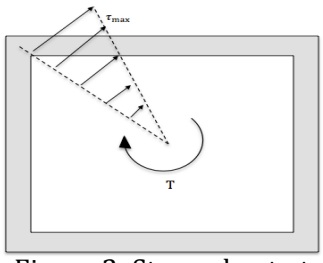

Figure 2: Stress due to torsion

A fourth major stress that was important to consider is the shear flow in the crane. While the elements of the beam might be able to withstand the shear force, connections between members will be in danger. Not only is the direct shear significant at all sections, but reactions to the torque from the tip load also causes large internal shears in fasteners. The yield limit of any individual rivet must not be exceeded.

With these stress characteristics in mind, we found several strategies employed in aircraft design to be useful to consider. A primary application for boxlift structures is in airplane wings. Modern aircraft are constructed primarily from sheet metal stretched over hollow frames, forming semi-monocoque structures [4]. Like the crane, the wings act as cantilevered beams subjected to bending from the lift force.

The principal structural members of airplane wings are spars that run parallel to the lateral axis of the aircraft [1]. These spars are integral to the design, as they bear the majority of span-wise bending, and give the most stiffness to the wing. In order to distribute stress, crosspieces called ribs are added to transmit load from the skin to the spars. Together the spars, sheet metal skin, and ribs form a box beam that gives the wing structural stability.

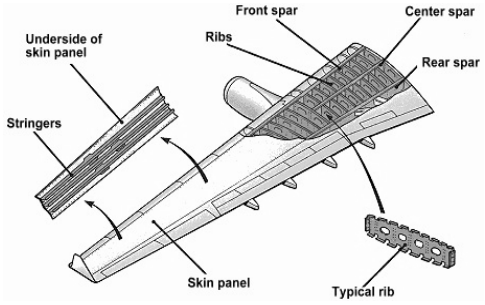

Figure 3: Assembly of airplane wing [3]

With this wing design as a motivation, we were able to design a boxlift crane with two main structural lengthwise spars connected by aluminum siding skins and ribs. This structure was intensively modeled in Creo Parametric and idealized to withstand high stresses due to bending as well as torsion. We followed the Colin Chapman mantra of "Simplify, then add lightness." Accordingly, excess material was then removed to reduce weight and pare the design down to its essential components.

The final design is presented below:

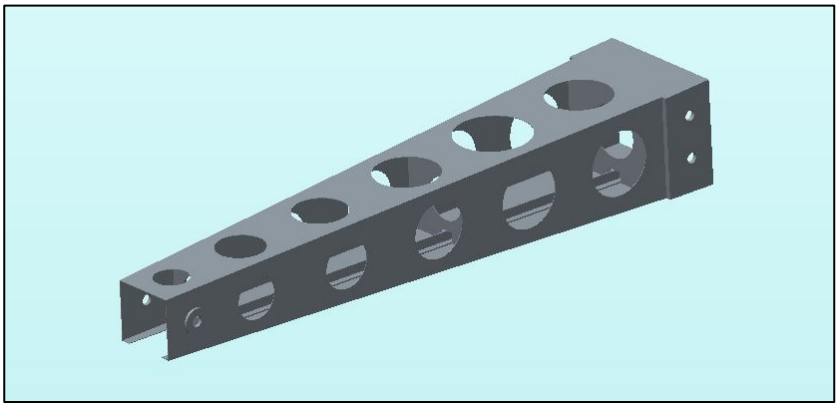

Figure 4: Boxlift Crane Design

II. Detailed Design and Analysis

A. Basic Design Approach

In designing the crane, the primary goal at each stage was to minimize overall stress. While the design specifications are relatively strict, and dictate that the general appearance of the boxlift be that of a tapered, hollow beam, there is still much room for analysis and optimization.

A first order of business in the design process was to choose the working materials. Then the material properties could be used in subsequent structural analyses. Faced with choices between the various categories of aluminum alloys, we mainly deliberated between 2024 aluminum and 6061 aluminum siding, including possible combinations of the two.

In the end we decided upon 2024 aluminum because of its superior strength and quality. Aluminum 2024 is very stiff, easy to machine, and has a higher failure stress than 6061 — rated at a yield strength of 45,000 psi, versus 35,000 psi for 6061 [7]. On the other hand, 2024 does not yield easily, and thus will apply more shear stress to the rivets. For the side panels that property was fine, as the rivet spacing could be easily condensed. However for the L-beams we chose aluminum 6061 so that it would lend some give to the structure.

To draft an initial sketch of the main parts of the crane, the beam mechanics outlined in the introduction were studied. Generating free body diagrams, shear diagrams, and moment diagrams allowed us to visualize the theoretical stress profile. While shear is constant, the magnitude of the bending moment increases linearly towards the root. Since the moment depends directly on the length of the beam, we chose to set the point where the beam is loaded to be at 28.5 inches, close to the minimum allowed distance from the column base. The overall length of the crane was set at 30 inches to give extra room between the loading sites and support pins from the ends.

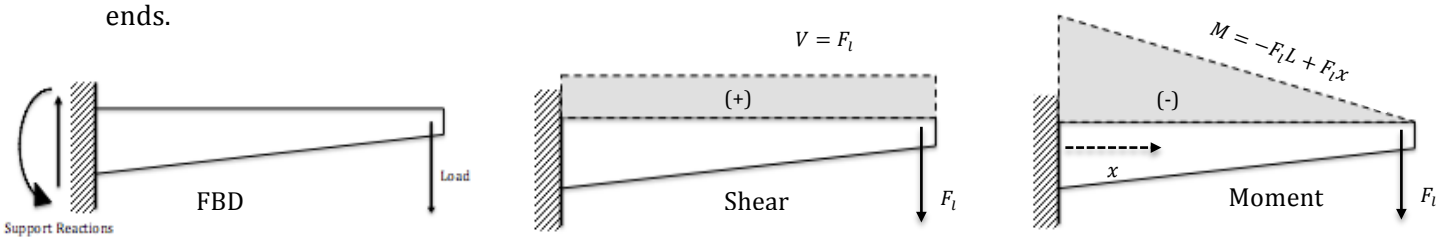

Figure 5: Free body, shear, and moment diagrams

To resist the large bending moment, the distribution of mass of the crane should be designed such that the moment of inertia about the neutral axis of the crane is maximized. The moment of inertia is defined as $I_{\bar{y}} = \int y^2 dA$, thus the taller the crane, the stiffer it will be. Similarly, the concentrated weight of L-beams used to join the sides together in the corners also increases *I*.

In terms of torsion, the polar moment of inertia is the value that is important. As the polar moment of inertia is defined as $J_O = \int r^2 dA$, both increasing either the width or height of the beam will help, as will the L-beams in the corners [5].

However, while the larger the structure is, the better it can resist stresses, it is not necessarily an optimal design. In order to fulfill the other goals of the project, the crane's weight must be minimized. Thus, finite element method studies must be performed to identify which dimensions allow for both the minimum weight and sufficient strength to avoid failure.

B. Optimization of the Boxlift Crane Shape

Having identified the need to analyze the tradeoff between ultimate strength and material usage efficiency, we turned to FEM tools in Creo Parametric to find ideal values for the tip width and height. Since the design specifications had multiple stringent constraints on size, the range of values to be tested in *Creo* was significantly reduced. With the beam length set at 30 inches, the maximum tip thickness limited to 3 inches, and the range of tip widths that satisfied the taper and

aspect ratio specifications contained between 3 and 3.25 inches, we ran static analyses, sensitivity studies, and optimization calculations on the crane model.

A static analysis in Creo takes in a structure and a set of constraints and loads and solves for the maximum stresses found in the piece. A sensitivity study takes the structure and modifies a user specified dimension — testing a range of different values to calculate what the max stress would be if the given dimension were that size. For our dimensional analysis we used general loads not specific to 500 lbs. The most relevant feature of the graph is its slope.

The sensitivity study performed on the beam tip height confirmed what our original design predicted. As the height increased so did the moment of inertia, and thus the maximum stress in the beam decreased. However, as seen in Fig. 6, there are diminishing returns. The height was optimized at 2.85" — near, but not quite equal to, the maximum allowable value of 3".

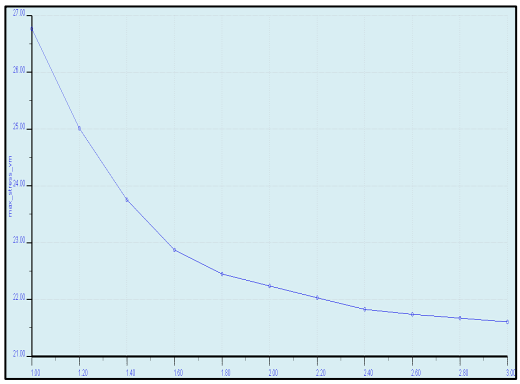

Figure 6: Sensitivity study on tip height under ½ chord loading

Similarly, the sensitivity study on the tip width yielded results that agreed with our analytical model. Increases in width increase both the polar moment of inertia as well as the moment of inertia about the neutral axis. However, a wider tip creates a larger torque when the 500-pound load is placed on the quarter chord, as seen by the positive slope of the sensitivity study for width under torsion. This meant that a steeper planform taper was beneficial for our design.

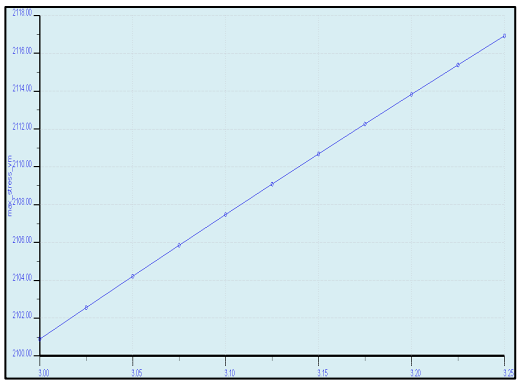

Figure 7: Sensitivity study on tip width under ¼ chord loading

In order to stiffen the bottom panel to help prevent buckling, we chose to include a lengthwise T beam. From Eq. (2) we know that increasing the cross sectional moment of inertia raises the threshold $P_{critical}$ for buckling. Since the T beam has a large *I*, it significantly bolsters the stiffness of the bottom skin.

C. Rivet Placement

The main consideration in placing the rivets was ensuring that the stresses did not become so great that the rivets sheared out of the plates or snapped in half. In the given assembly, each rivet is subjected to both a direct shear force due to the shear flow in the aluminum plates and a resultant internal shear force due to the moments applied to the rivets by the cantilevered loading [6]. For a given rivet the shear is given by the following equation:

$$F_{shear} = \frac{V}{n} + \frac{Pe}{\sum {r_i}^2} r_i \quad (4)$$

Where V is the shear force at the section, n is the number of rivets distributing the load, Pe is the applied torque ($load\ P\ X\ lever\ arm\ e$) on the centroid of the fastened region, and r_i is the distance of the rivet to the centroid of the region.

Any specific rivet has a definite yield strength equal to some σ_Y. Thus, the maximum shear that a rivet can withstand before it fails is given by:

$$Max\ applied\ shear\ force = F_{max} = \sigma_Y \left(\frac{\pi d^2}{4}\right) \quad (5)$$

From equations (4) and (5) it is clear that total rivet load capacity depends on three main variables: the number of rivets, the stress-strain properties of the rivets, and the diameter of the rivets. Researching on McMaster-Carr, we ordered two types of rivets: one with shear strength of 120 lbs, and a second high-strength rivet with shear strength of 700 lbs.

To calculate the sufficient rivet placement at each section of the crane total shear force calculations were done in excel for each rivet. As expected, it was found that the rivets on the side

mounts experienced the greatest stress since at that point the torque Pe is maximized. Thus, the high-strength rivets were used, and the rivets were placed such that net F_{shear} was minimized while at the same time still ensuring that each part of the side mount was secured.

Additionally, it was found that the rivets on the side skin experienced greater rivet shear force at the ends, and less at the center. However, it was low enough at all places to allow us to use the standard rivet with shear strength of 120 lbs.

D. Structural Analysis with FEM

With the general shape and structure of the boxlift crane decided, Creo's finite element methods for stress testing were used to meticulously study the performance of the crane under the actual design load. When the 500 lb force was applied to the beam, we were carful to check for areas that were under strains that exceeded the material limits of aluminum.

The primary analyses of the beam under 500 lbs applied at the mid-chord revealed that the greatest stresses occurred at the pin connections to the test-bed column. At the holes, large horizontal forces would cause the pins to tear out of the thin aluminum sheets. This area was clearly the weakest spot in the crane.

The forces in the pin supports are so large since they are the sole providers of moment and vertical force balance in the crane. While the vertical force F_y in one hole of one of the support plates is significant at 125 lbs, the horizontal force F_x is much greater yet — 3,560 lbs for our design dimensions and d = 2 inches, the pin separation length on the test-bed column.

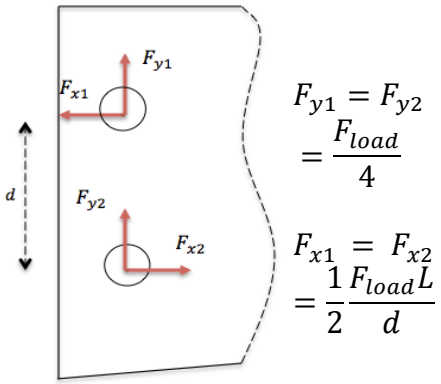

Figure 8: Pin Hole Forces

The main method of resolving this issue was to fasten thicker reinforcement plates of 2024 aluminum to the side panels at the pin holes. While the forces remain the same, the extra material reduces the overall stress. Optimization analyses were performed to calculate the ideal size and thickness for the plate.

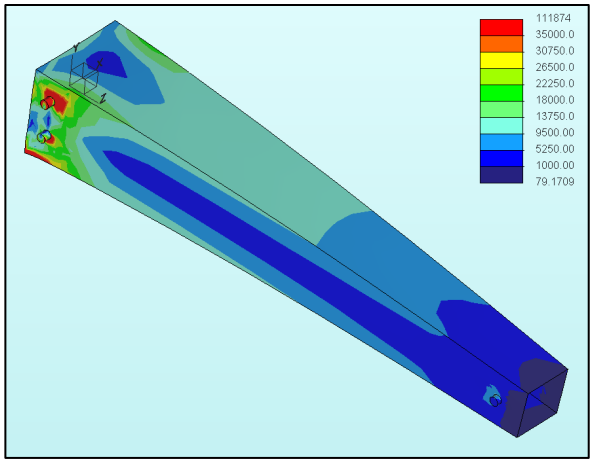

Figure 9: Von Mises stresses (psi) in the beam model without support plates.

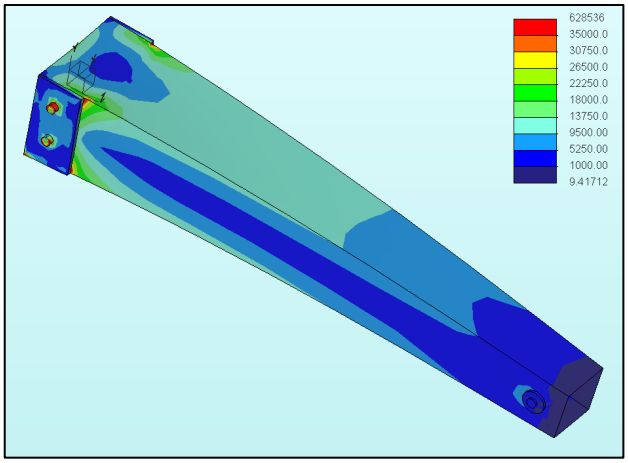

Figure 10: Von Mises stresses (psi) in the beam model with support plates.

The secondary analyses of the beam under torsion from 500 lbs applied at the quarter-chord showed that the crane needed to be stiffened substantially. While the design was able to withstand direct bending, the addition of a torque caused the crane to fail. Asymmetric stresses in the skin from the off axis loading caused the side spars to twist and buckle. In order to stiffen the structure and resist the torque, square plate ribs were added to span the crane between the side spars.

These ribs added stiffness to the crane due to their large polar moments of inertia, and being attached to the sides of the crane allowed them to distribute concentrated stresses through the whole structure. With each rib addition, the stresses in the crane diminished considerably. In particular, the ribs had the biggest effect on the strains at the ends of the beam where the reaction forces are. Additionally, not only did the ribs reduce the maximum stress, but they also proved to be very effective in maintaining an even stress profile throughout the structure. Our analysis led us to place three ribs in the crane — one at the root, one at the midsection, and one at the tip. In order to reduce weight and to allow for the pulley cable to pass through the center of the crane, the centers of the ribs were hollowed out.

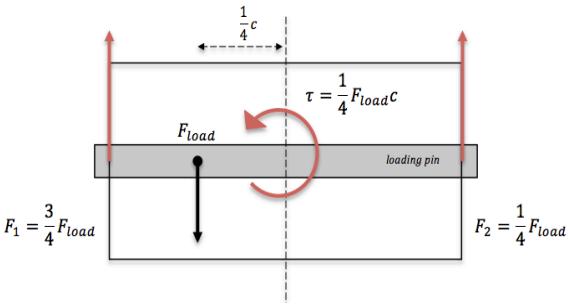

Figure 11: Cross sectional view of reaction forces due to ¼ chord loading

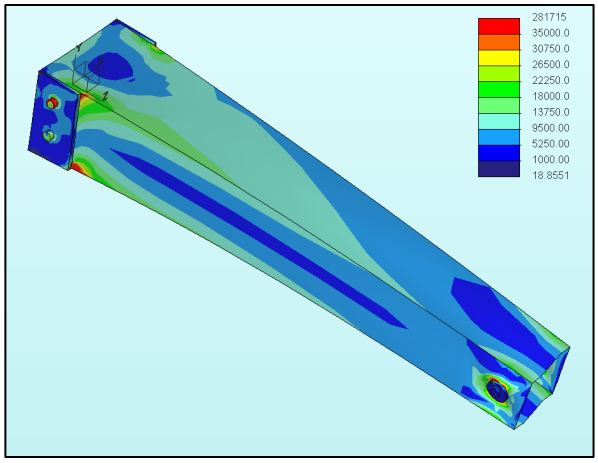

Figure 12: Torsional stresses (psi) in the crane with no cross sectional bracing. Note the distinctly asymmetrical stress profile.

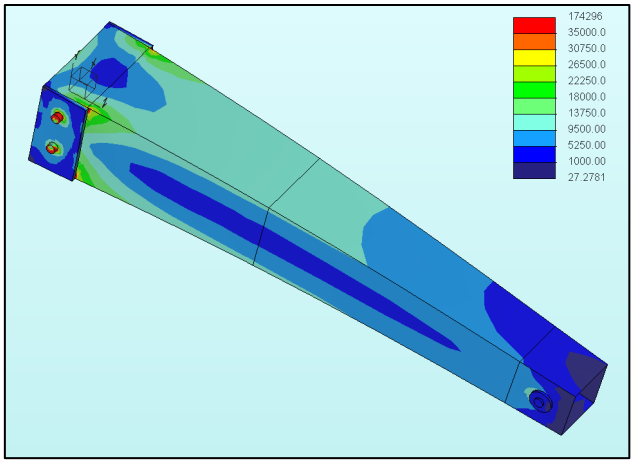

Figure 13: Torsional stresses (psi) in the crane with the addition of ribs. Note the reduced stress at the root and tip and the even stress profile.

In addition to analyzing the crane as a whole, a closer analysis on the stability of the bottom panel with respect to buckling was performed. Without any type of reinforcement, the plate buckled easily. When the T-beam was added the stiffness of the plate increased dramatically. Finally, once the ribs were added in, they reduced the effective length, and the crane was further fortified against buckling instability.

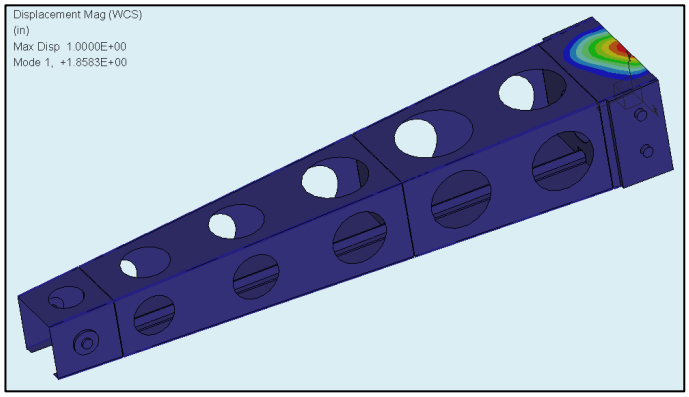

Figure 14: Buckling in the crane was avoided for loads up to and including 760 pounds force, where we believe the rivets will fail.

E. Weight Reduction

Once the problematic stress issues were resolved in the crane structure, no one area was above the failure limit of the material. However, the stress distribution was certainly non-uniform. Some sections of the crane were practically in a state of no stress compared to the most strained areas. In terms of efficiency, a lot of the material in those lightly loaded areas was wasteful. Once these low-stress areas were identified, we could remove material to reduce weight without compromising the structural integrity of the crane.

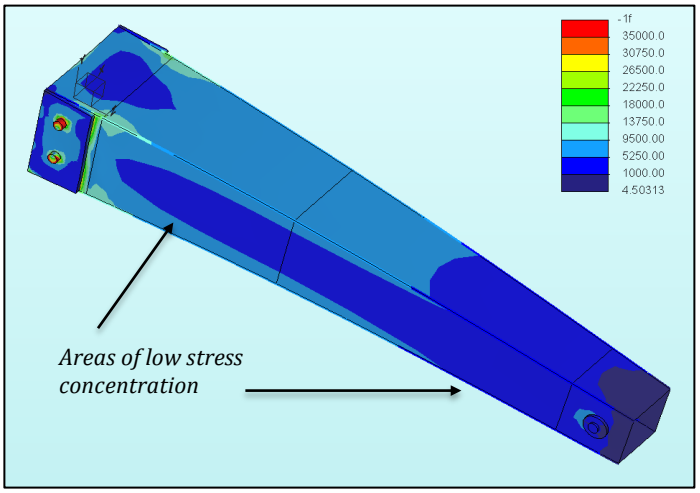

Figure 15: Identification of areas of low stress (psi) in loaded crane.

The process of removing material from the crane skin was not trivial. An additional important consideration in cutting away from the aluminum was to perform it in a way such that stress concentrations would not be induced. Stress concentrations are formed when the area of a loaded member reduces sharply [5]. The worst sources of highly concentrated stresses are sharp angles, such as in squares or triangles. Thus, to minimize the introduction of stress risers we chose to cut out the only circular holes from the material. While ellipses might also have worked, circular holes are much simpler and quicker to manufacture. Using Creo's analysis tools, the spacing and sizing of the holes were optimized.

Once the design of the holes for weight reduction was completed, we reran the failure tests for bending, torsion, and buckling to verify that the crane was still just as structurally sound. While the stresses inevitably increased, they were still well within safety limits.

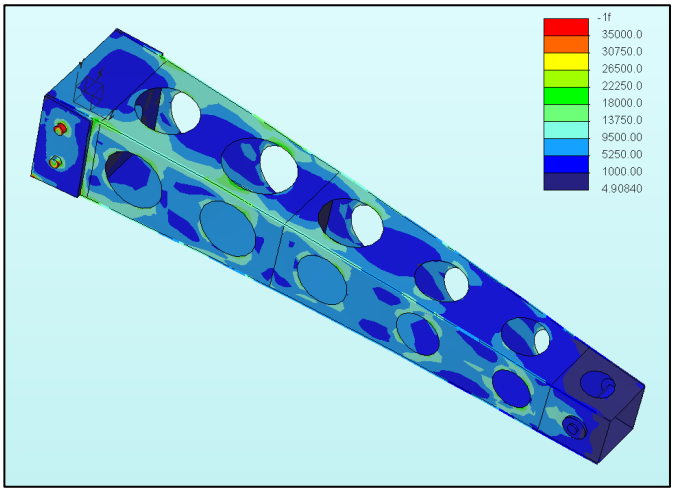

Figure 16: Stress profile (psi) in weight reduced beam when loaded on the ½ chord

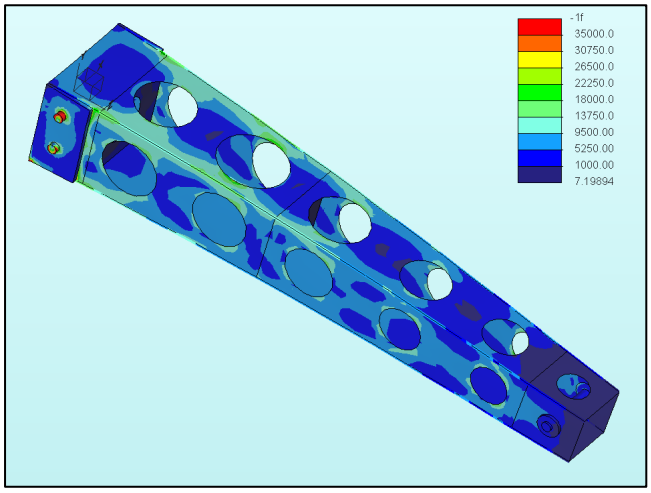

Figure 17: Stress profile (psi) in weight reduced beam when loaded on the ¼ chord

F. Failure Prediction

While our analyses give us confidence that our crane will withstand the test load of 500 pounds, all structures have an ultimate yield and failure strength. If the crane is to fail, our prediction is that the weak link will be the rivet fasteners. Since the 2024 aluminum used in the skin is very stiff and strong, it is more likely that rivets will snap due to shear than the skins failing from large deformation. In fact, we predict that the beam will hardly yield at all.

To provide an estimate as to what specific load limit the crane can hold, we made slight modifications to the rivet calculations done in (II. *C.*) to find the maximum shear that the rivets would hold before popping out of the structure. For the side skins with rivets that had shear strength of 120 lbs, the load was limited to:

$$P_i * b = \left(\frac{Pe}{\sum r^2} * r_i + \frac{P}{n}\right) * b < 120\ lbs \tag{6}$$

With all the rivets placed, the load P was slowly increased until the shear forces reached approximately 120 lbs. The calculations were all done using excel. It was found that the maximum applied load that one of the side skins could handle was ≈570 lbs. Because there are two side skins, it is assumed that the load is distributed between the two skins. When the load is in the middle, each skin is assumed to hold half the load. However, during the torsion test, the weight is ¼ L from one of the skins where L is the distance between the skins. Thus the weight distribution will not be evenly divided in half. In fact, we calculate that to produce the equivalent moment, the the skin closest to the load will hold ¾ of the weight. Therefore if the skin could handle an applied load of 570 lbs before the rivets shear out of the skin, the structure can handle ≈760 lbs.

The same procedure was repeated to find out under what applied load the rivets in the side mount would shear out. As discussed earlier, larger rivets with shear strength of 700 lbs were used because the expected stresses on the side mount are much higher. Therefore:

$$P_i * b = \left(\frac{Pe}{\sum r^2} * r_i + \frac{P}{n}\right) * b < 700\ lbs \tag{7}$$

However, in the case of the side mount, the distance to centroid values, r, are much smaller and there are fewer rivets, because the mount is much smaller in terms of area than the side skin. However, because of the increased shear strength of the rivets, it was found that the structure could handle ≈ 920 lbs before the rivets in the side mount would shear out of the plate.

By this preliminary analysis, it would seem that the structure would fail once the load reached 760 lbs, at which point the rivets in the side skin would shear out. Because the top rivet closest to the base is furthest from the centroid, it will experience the highest shear stress. Therefore we predict that this rivet (or a near neighbor) will pop out first, leading to a decrease in the integrity of the other connections and causing the line of rivets to pop out.

To confirm that this would be the mode of failure, analysis was done in Creo with an applied load of 760 lbs. It was observed that the rivets would fail before the crane fails in any other way.

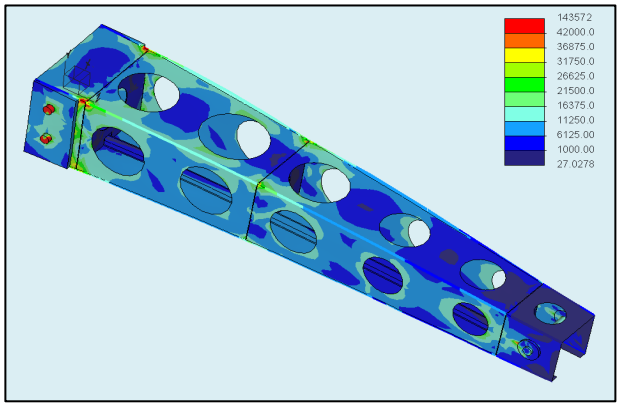

Figure 18: Applied load of 760 pounds force. (psi).

III. Conclusion

Our goal was to design an aesthetic, lightweight, and functional boxlift crane that met or exceeded all specifications and demands. As analyzed, the product that we designed and manufactured meets these criteria. Our crane is light and efficient; it weighs only 2.6 pounds, which is almost 15% below the weight limit. Symmetrical, crisp and clean lines make the structure pleasing to the eye, while minimally complex cuts reduced the difficulty of manufacturing.

While traits such as visual appeal and weight are important in the ultimate marketability and functionality of our crane, our primary focus was on performance. First we identified the key stresses and potential modes of failure with simple solid mechanics. Then, through our design process, we manipulated the critical geometrical properties that affected the strength limits of our crane.

While analytical calculations guided the groundwork for our crane design, extensive finite element analysis in Creo Parametric gave us specificity where hand calculations could not. With FEM we were able to optimize the tapers on both the sides and top, and were able to identify and strengthen critically weak areas. In order to resist twist due to torsion, we added cross sectional ribs that distributed the stress over the structure, and thus gave extra rigidity to the crane. Additionally, Creo proved especially useful in identifying which areas of the aluminum skin were in states of high stress and low stress. Using this information, we were able to cut material from structurally unimportant areas, and thus meet our objective of minimizing weight while maintaining high performance.

In principle, our crane could be prototyped, tested, and further refined; here we relied on computational techniques to demonstrate that our crane will withstand the assigned loads. In order to thoroughly validate our design, an exhaustive simulation based testing was performed. With 500 pounds acting on the ¼ and ½ chords our crane displayed stress levels well below the material limits of aluminum 2024. Bending, torsion, and buckling tests were performed, with care taken to check for small concentrated areas of stress, as well as general failure patterns. In order to maintain the legitimacy of our test results, we had to take caution to machine the true parts as close as possible to the model. We are confident that our craftsmanship did not introduce any unforeseen weaknesses or imperfections to any appreciable degree.

If the crane were eventually to collapse, the expected mode of failure would be shearing of the rivets. Since the side skins are so unyielding, the shear stress in the rivets will exceed their yield strength well before the skin fails. When a rivet fails, the force that it was carrying falls over on the neighboring rivets. Hence once the first connection gives, the remaining seam of rivets is likely to unzip. While this is how we predict our crane will ultimately fail, we anticipate that this will not happen until the loading approaches 750 – 800 pounds. We are confident that at the expected load of 500 pounds our crane will be safe and structurally stable with deflections well below four inches.

IV. References

[1] Chintapalli, Sridhar. "Preliminary Structural Design Optimization of an Aircraft Wing-Box." *SPECTRUM Research Repository*. Concordia University, n.d. Web. 24 Oct. 2013. <http://spectrum.library.concordia.ca/9093/1/MR20758.pdf>.

[2] "Aircraft Structures." *Aviation Maintenance Technician Handbook - Airframe*. Federal Aviation Authority. Web. <http://www.faa.gov/regulations_policies/handbooks_manuals/aircraft/amt_airframe_handbook/media/ama_ch01.pdf>.

[3] "Airbus Airplane Wing Structure and Terminology." *Nomenclature, Teardown, Exploded Diagram*. N.p., n.d. Web. 24 Oct. 2013. <http://www.nomenclaturo.com/airbus-airplane-wing-structure-and-terminology.html>.

[4] Peery, David J., and Jamal J. Azar. *Aircraft Structures*. New York: McGraw Hill, 1982. Print.

[5] Hibbeler, R. C. *Mechanics of Materials*. Upper Saddle River, NJ: Prentice Hall, 1997. Print.

[6] Megson, T.H.G. "Connections." *Aircraft Structures*. 407-15. Web.

[7] "McMaster-Carr." *McMaster-Carr*. N.p., n.d. Web. 24 Oct. 2013.

V. Acknowledgements

It should be noted that everyone contributed comparable amounts of work to this project.

Gabriel Baraban: Preliminary research, Creo simulations and initial design, parts drawings for report, torsion rib design and Creo modeling, report editing. Manufacturing: Side support plates and ring pin rivet holes, along with general assistance.

David Beck: Preliminary design, torsion rib simulation and analysis, production of Creo simulations and figures used in report, report editing. Manufacturing: Cut side skins, assisted in machining and side plate hole adjustment.

Annie Cardinal: Group leadership, organization, scheduling and logistics. Ordering and selecting materials. Initial design, Creo simulations and CAD work, report editing. Manufacturing: Primary manufacturing and assembly, milling and countersinking of side support plates with angled backing, riveting and drilling for crane assembly, final polishing, fitting and sanding.

Richard Cheng: Initial design, Creo simulations, and CAD design. Rivet calculations, spacing, specific placement in parts and CAD drawings, and selection of rivets for use in crane. Failure predictions for report along with final editing. Manufacturing: Final polishing and Dykem removal.

Adam Fisch: Primary Creo shape optimization, analytical mechanics research for report. Report: Primary writing, formatting, and editing of the report, including FBDs and other figures. Machining: Side skins and holes in side skins, laid out rivet holes, lathed ring supports.

Sebastian Grimberg: Preliminary research, design, and Creo simulations. Determination of form factor and shell shape. Manufacturing: Primary manufacturing and assembly, side skin layouts, cut circles in skins, drilling and riveting crane, designing and installing ribs, final polishing and grinding, cutting of L and T beams.

Po Wah Moon: Initial design, Creo simulations, and CAD design. Rivet calculations, spacing, specific placement in parts and CAD drawings, and selection of rivets for use in crane. Failure prediction for rivets and general Creo work. Report editing.

We pledge our honors that we have not violated the Honor Code on this project.

VI. Final Design Drawings and Renderings

The following series of pages are CAD drawings and 3-D renderings of our individual crane elements. Drawings are to scale, as noted.

Drawings include:

1) Full assembly
2) Side skin
3) Bottom skin
4) Top skin
5) Left support plate
6) Right support plate
7) Base rib
8) Middle rib
9) End rib
10) Ring Supports

Full Assembly

All units in Inches

Scale .25 unless noted

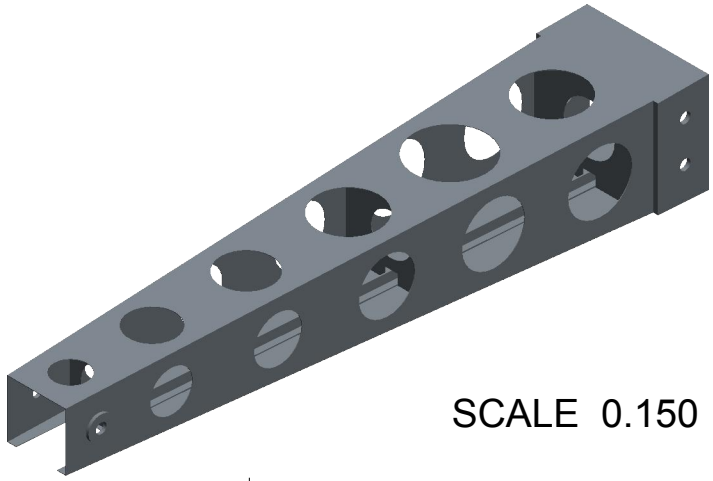

SCALE 0.150

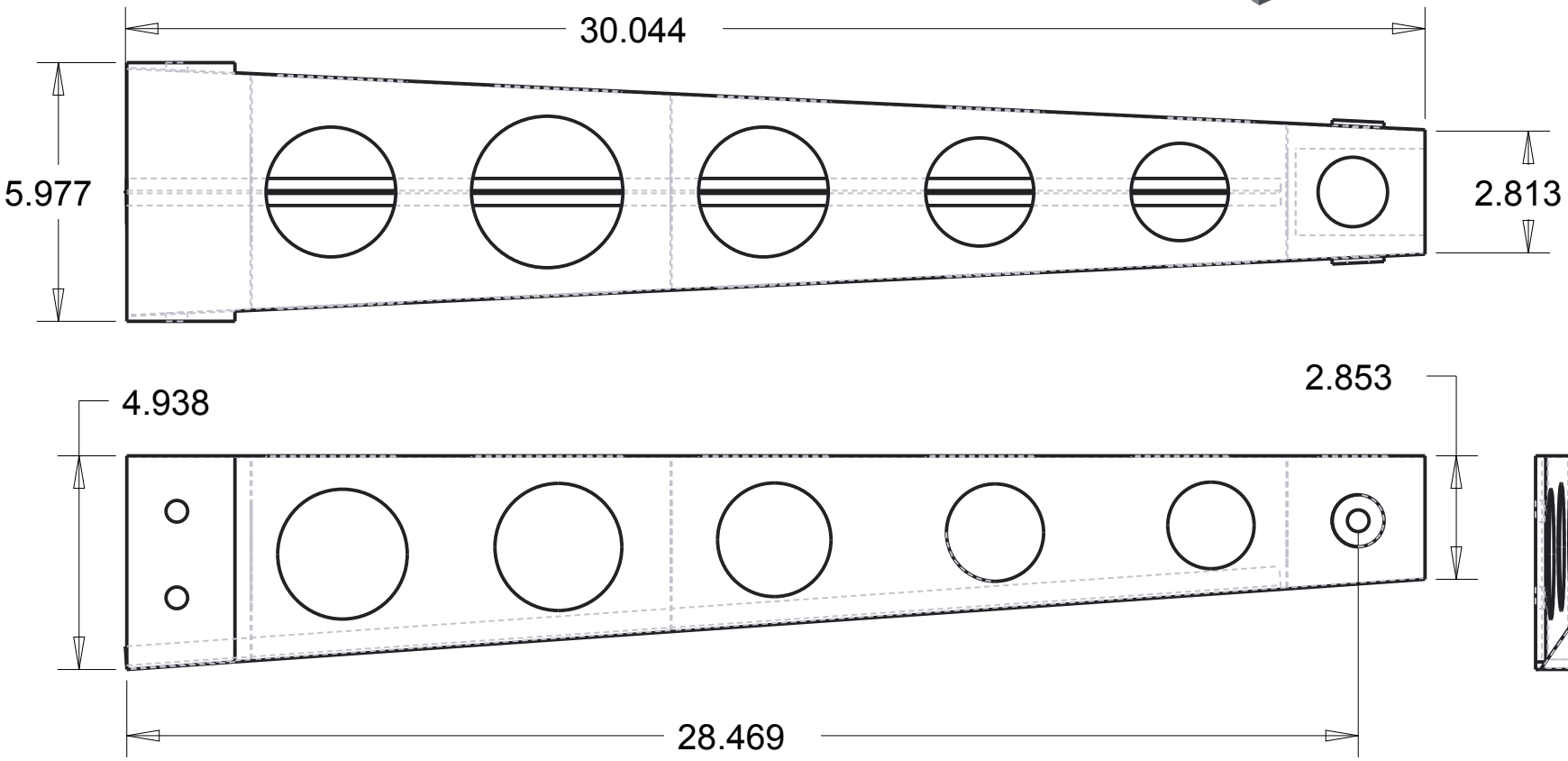

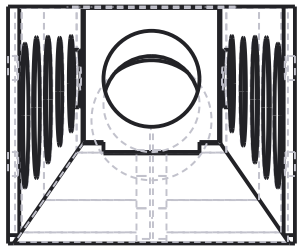

Side Skin

2 Required: 2024 Aluminum

All Units in Inches

All scales .25 unless noted

Riveting diagram attached at 1.25 scale (cropped)

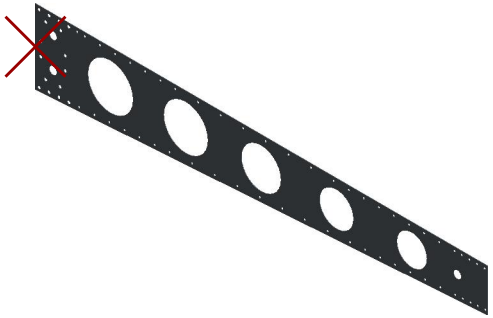

SCALE 0.111

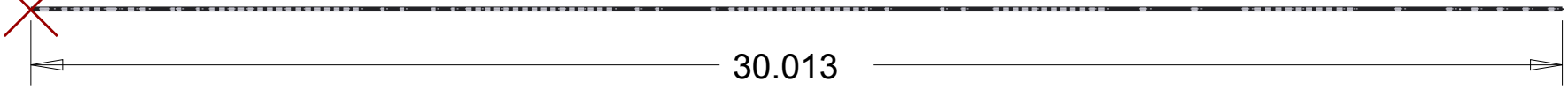

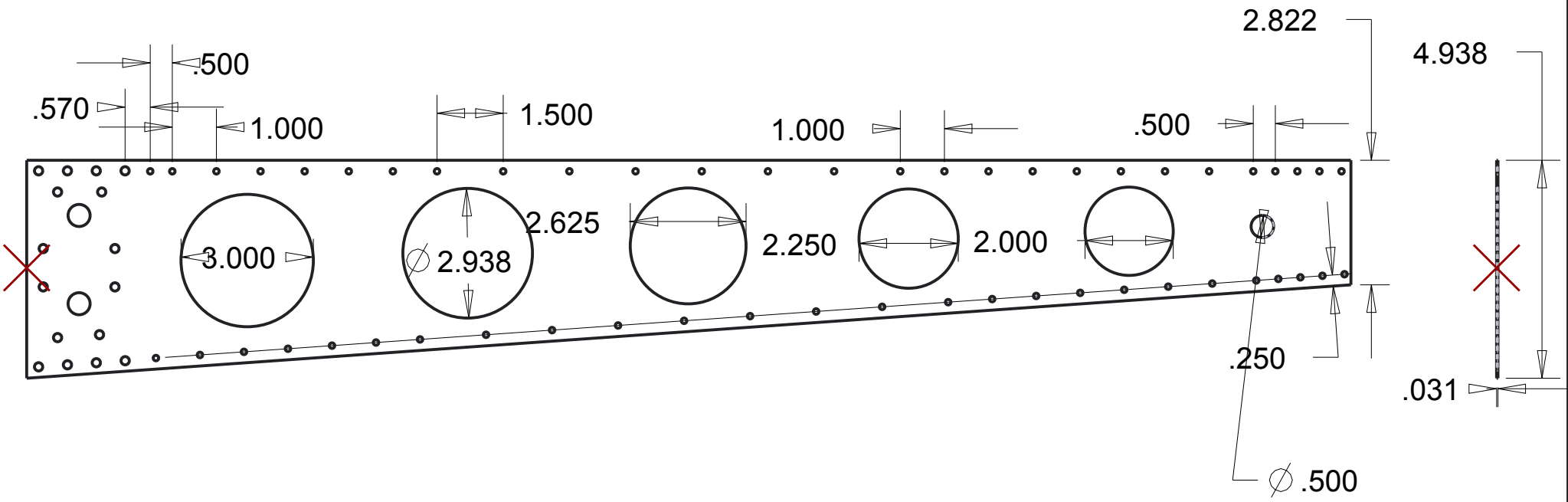

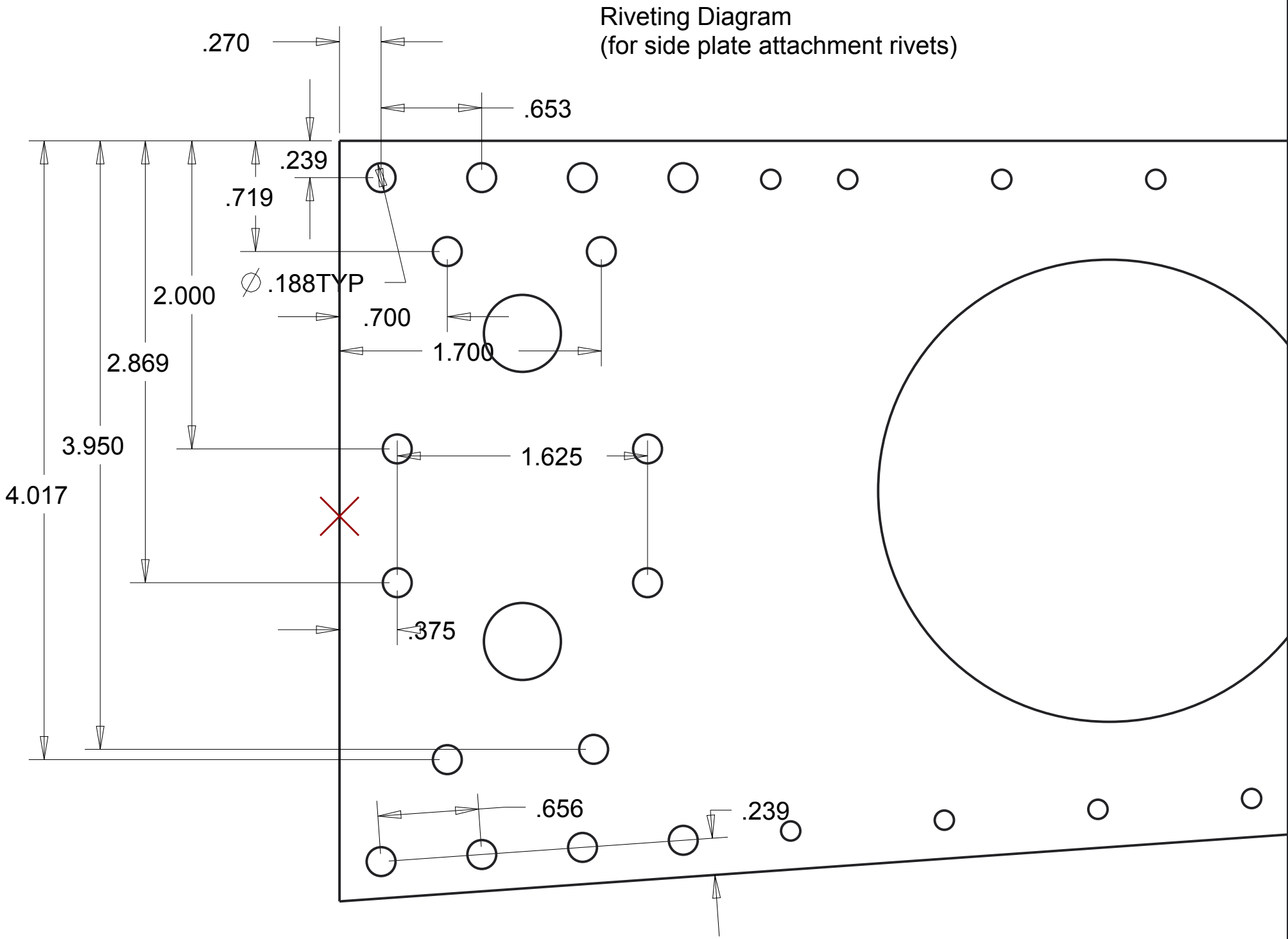
Riveting Diagram
(for side plate attachment rivets)
.270
.653
.239
.719
∅ .188TYP
2.000
.700
1.700
2.869
3.950
1.625
4.017
.375
.656
.239

Bottom Skin

1 Required: 2024 Aluminum

All Units in Inches

Scale 0.25 unless noted.

The rivet holes are symmetric, and only the left most value is shown for each region of different spacing.

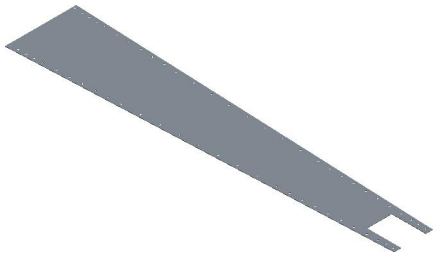

SCALE 0.091

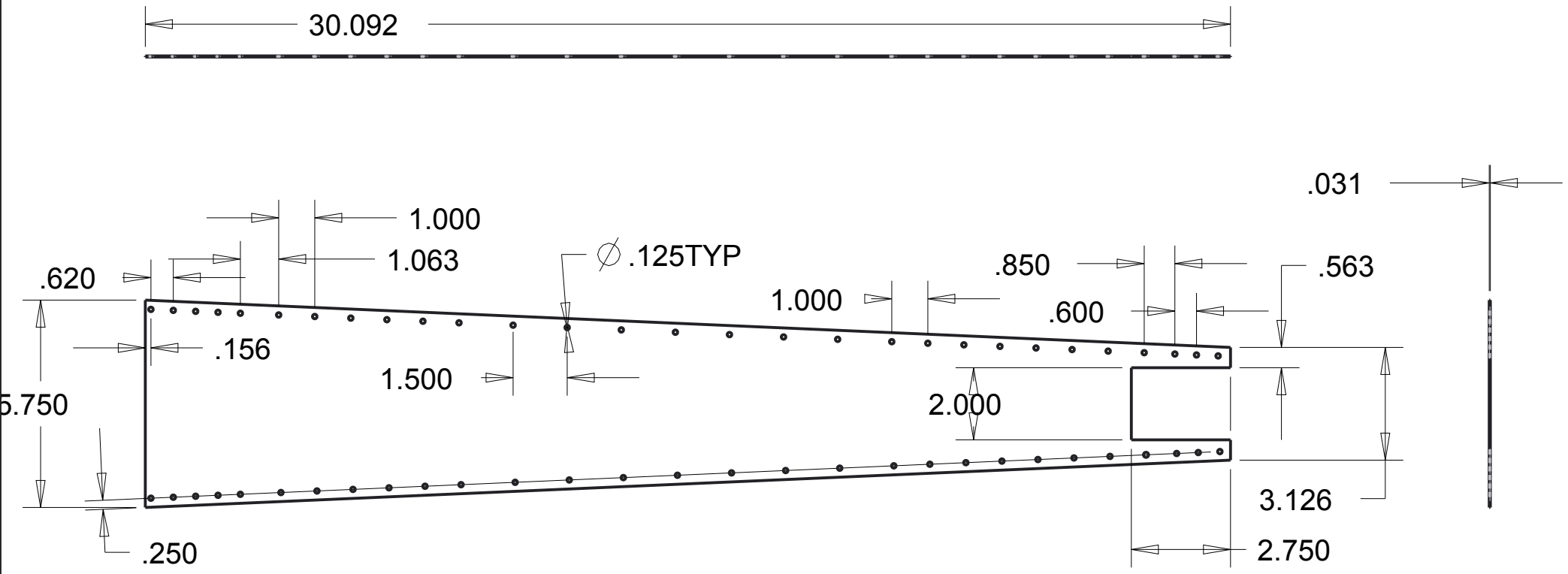

Top Skin

1 Required: 2024 Aluminum

All units in Inches

Scale: 0.25 unles noted

Only the left most rivet spacing of each group is listed

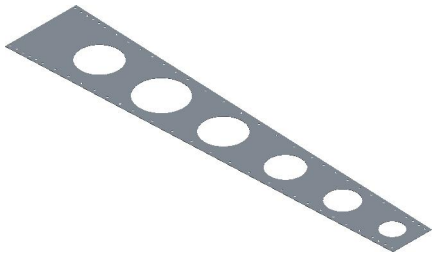

SCALE 0.091

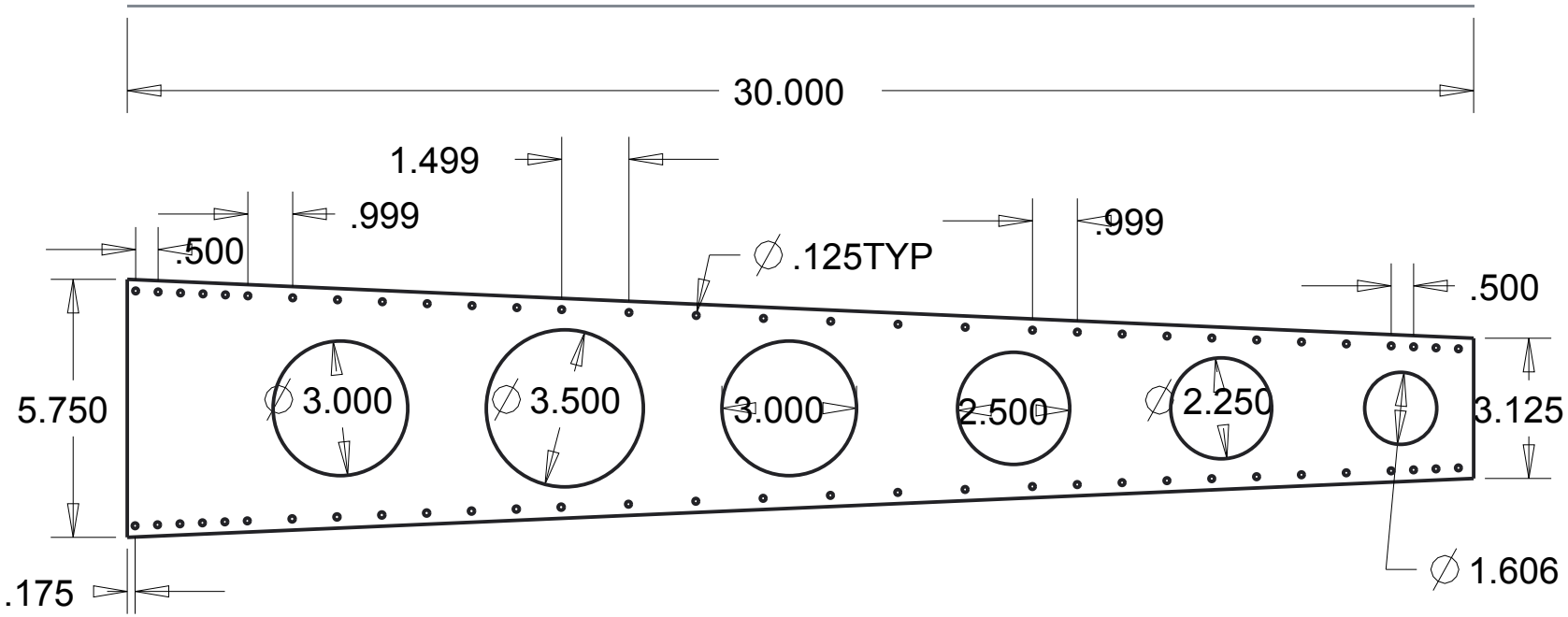

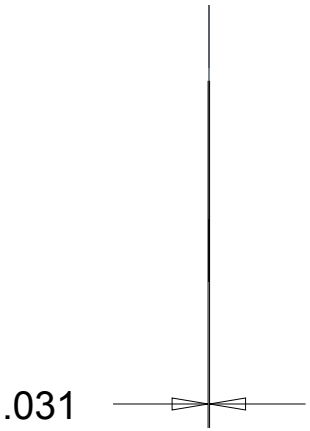

Left Support Plate

1 Required: 2024 Aluminum

All Units in inches

Scale 1:1 unless noted

SCALE 0.250

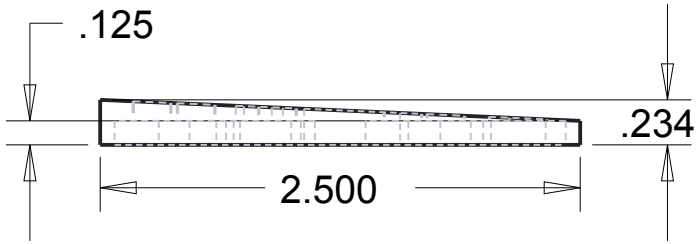

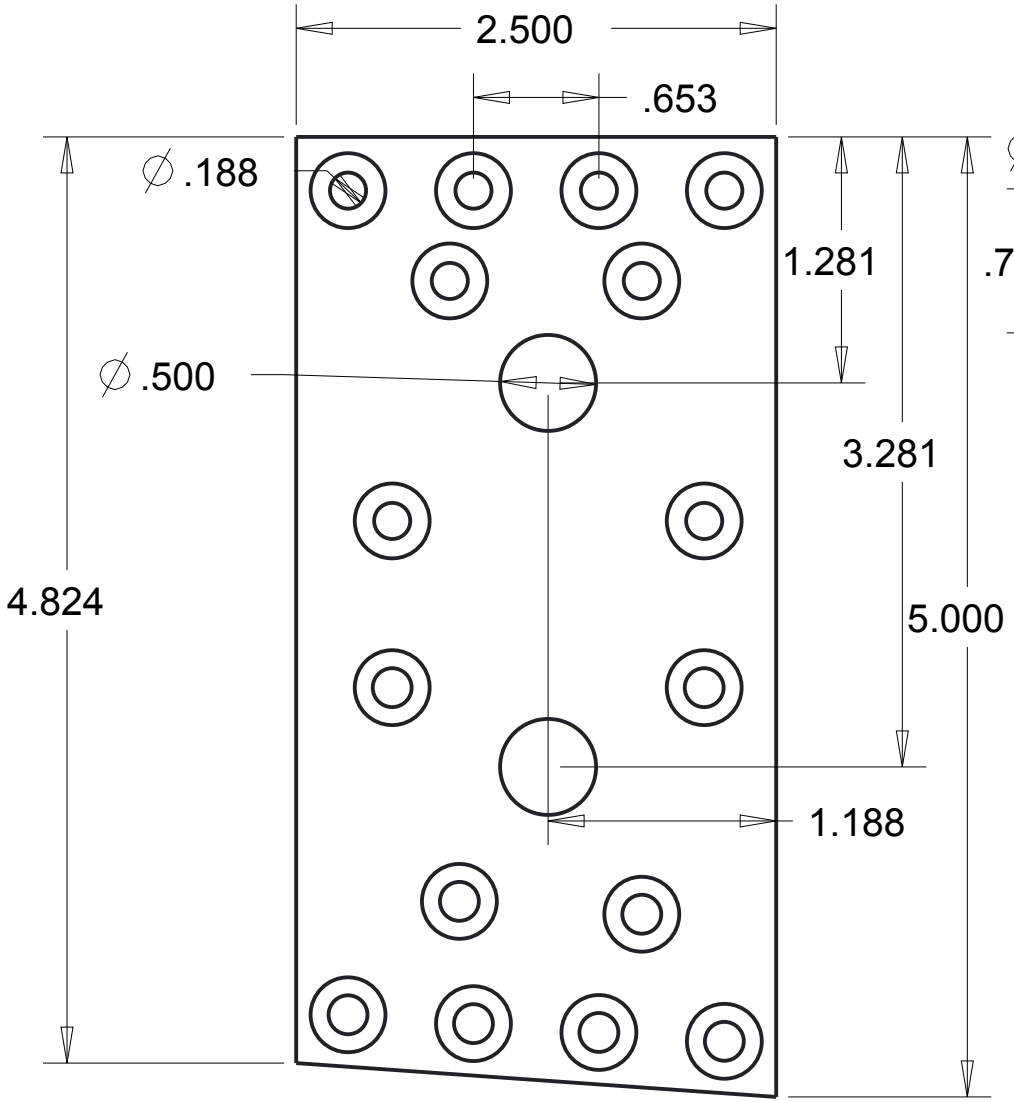

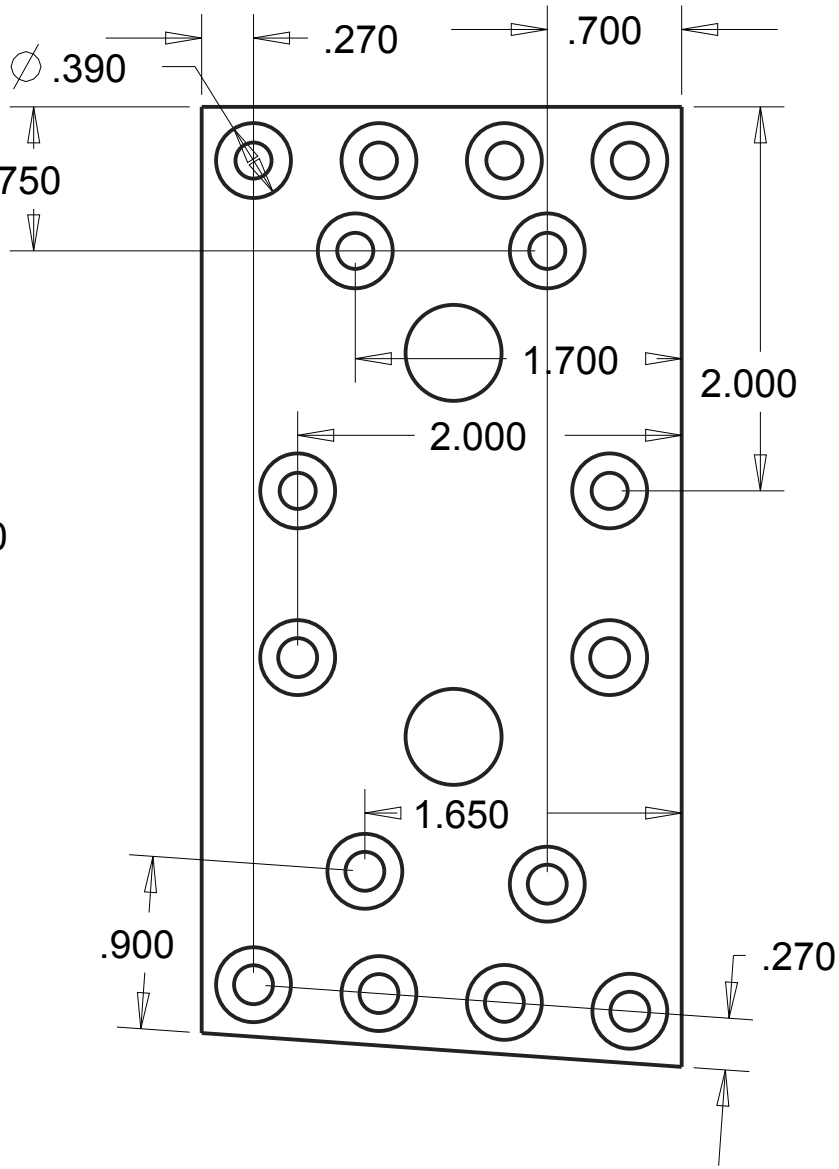

Right Support Plate

1 Required: 2024 Aluminum

All Units in inches

Scale 1:1 unless noted

SCALE 0.250

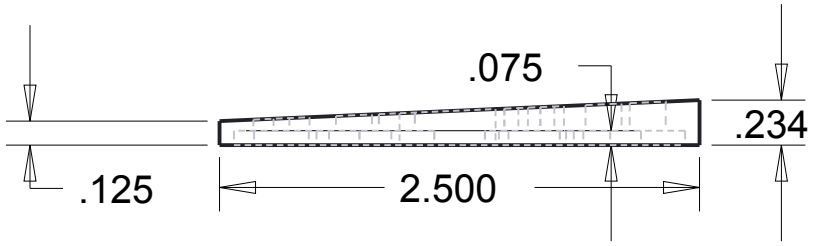

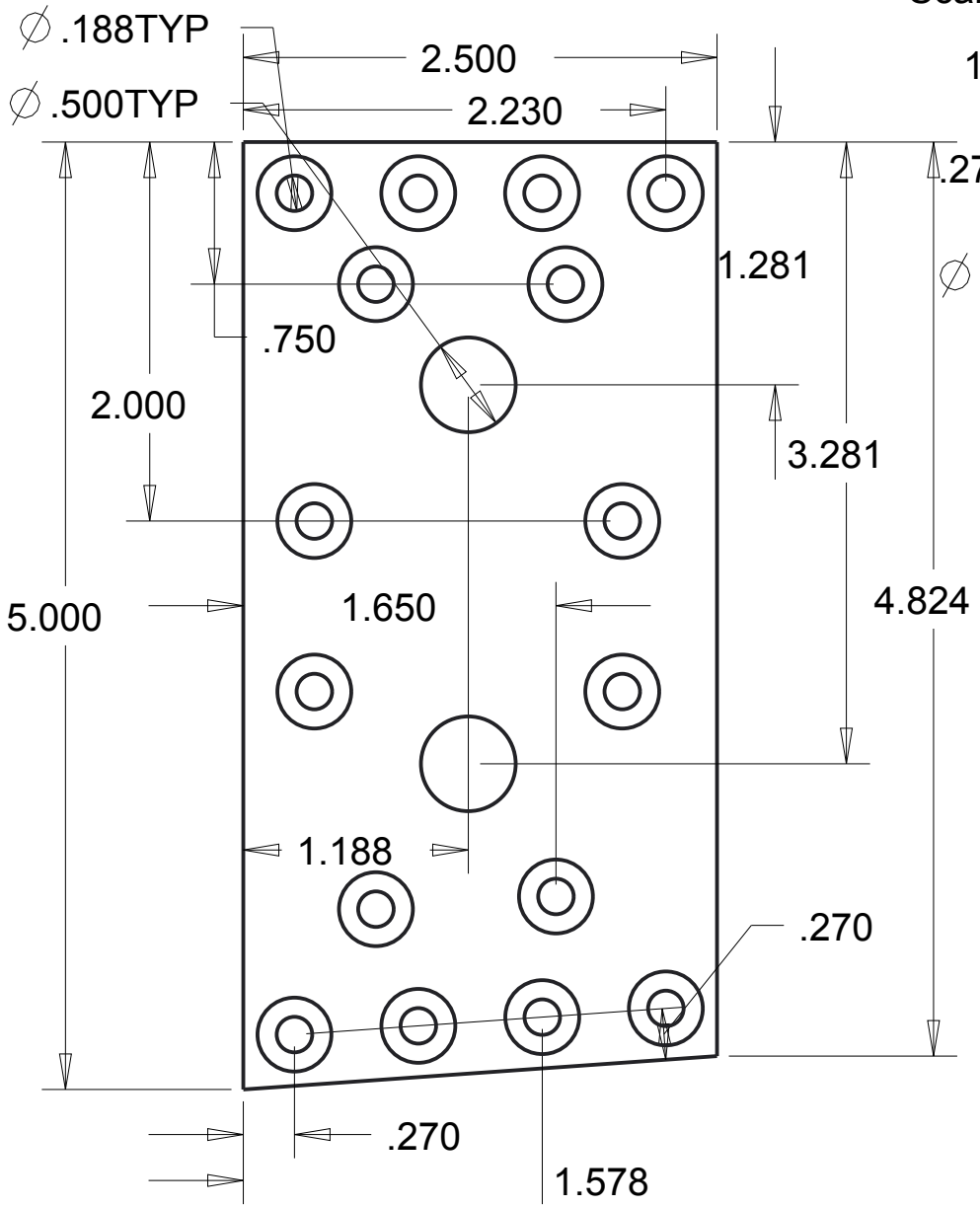

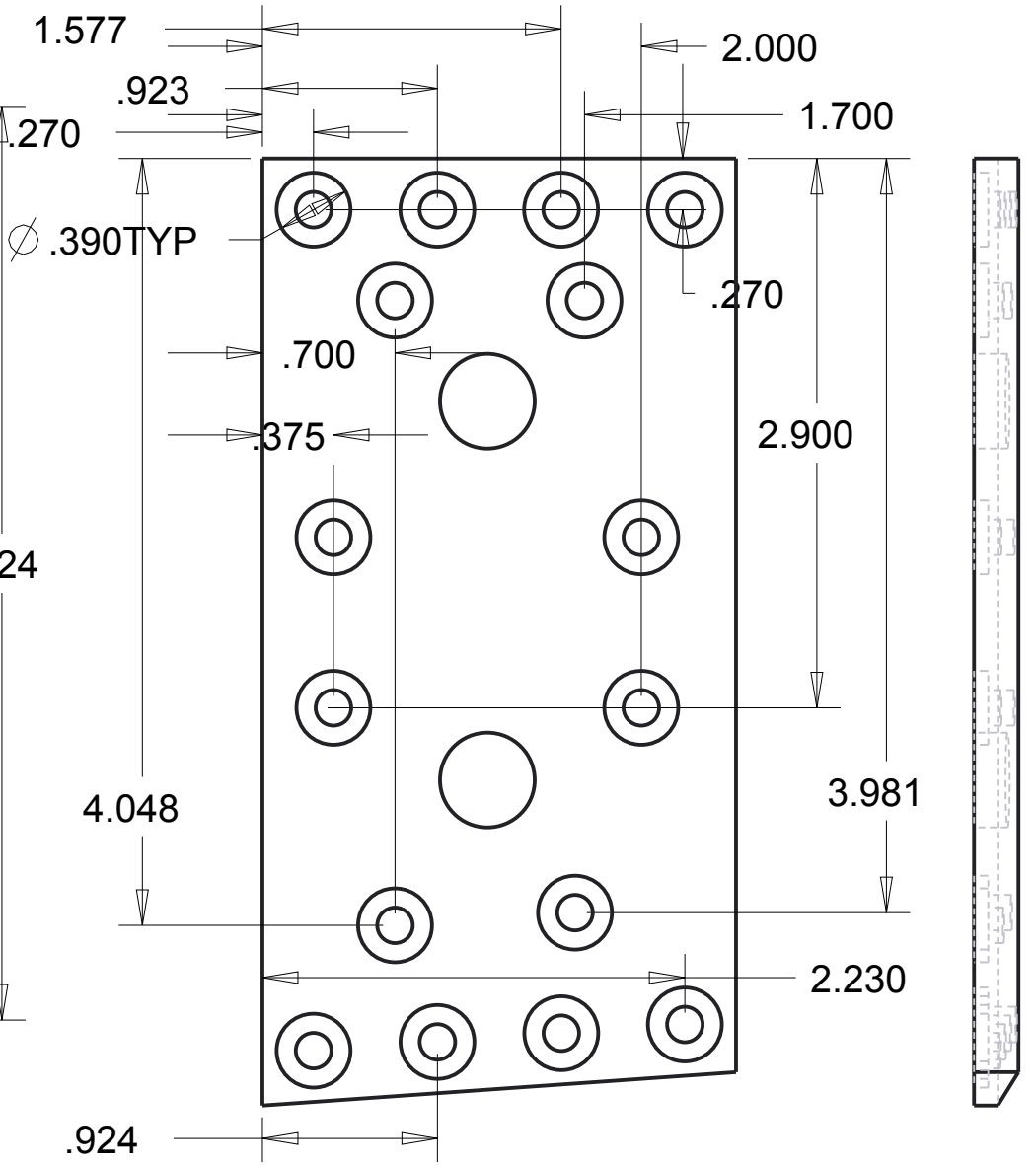

Base Rib

1 Required: 2024 Aluminum

All Units in Inches

Scale .5 unless noted

Fold tabs to form rivet flaps.

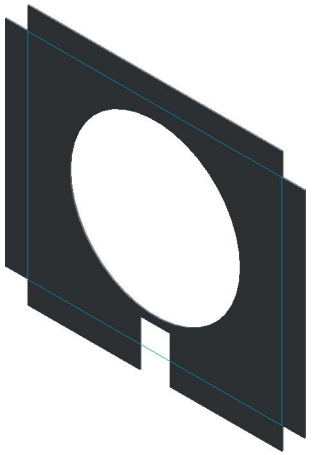

SCALE 0.333

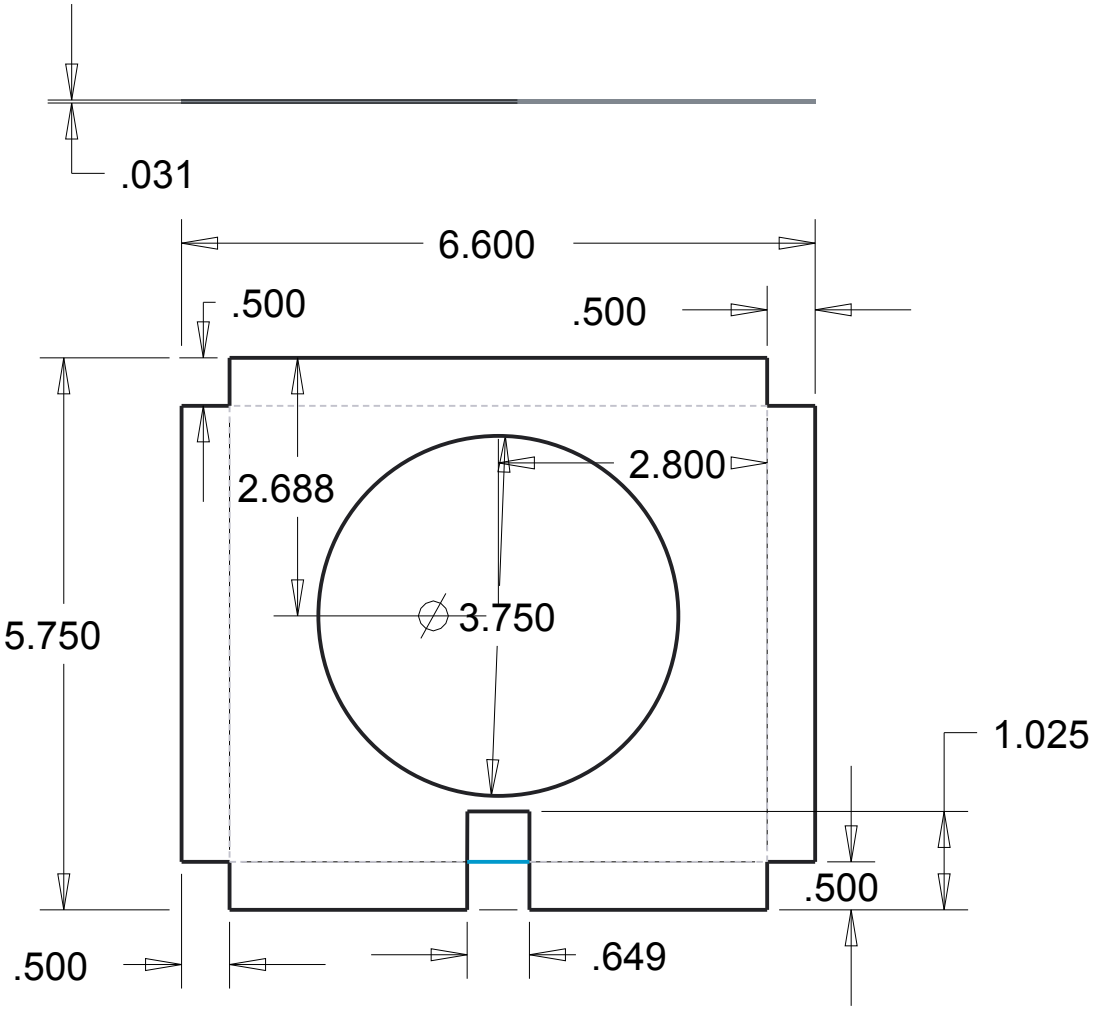

Middle Rib

1 Required: 2024 Aluminum

All Units in Inches

Scale .5 unless noted

Fold Tabs to create rivet flaps

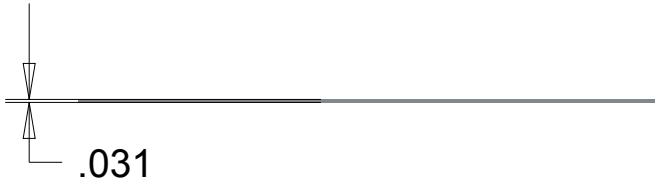

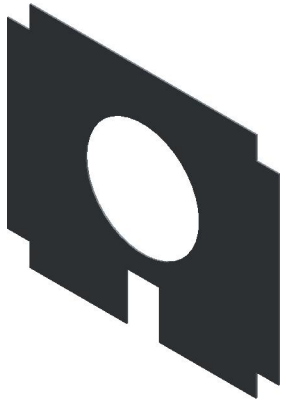

SCALE 0.333

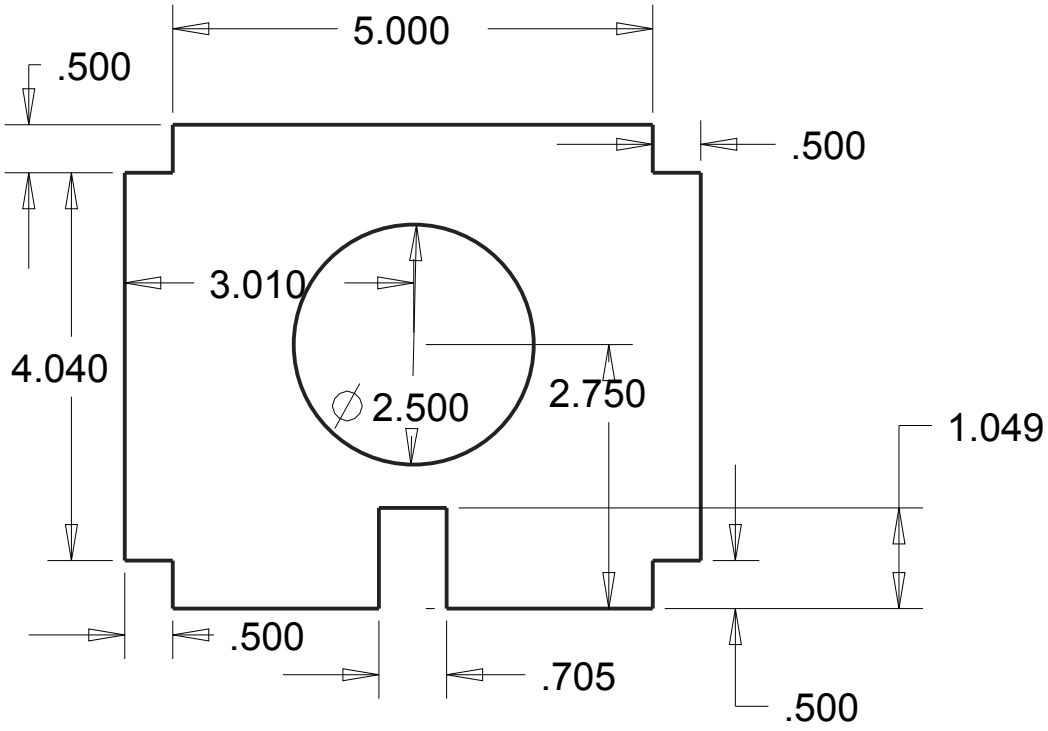

End Rib

1 Required: 2024 Aluminum

All Units in Inches

All Scale 1:1 unless noted

Fold tabs to make rivet flaps

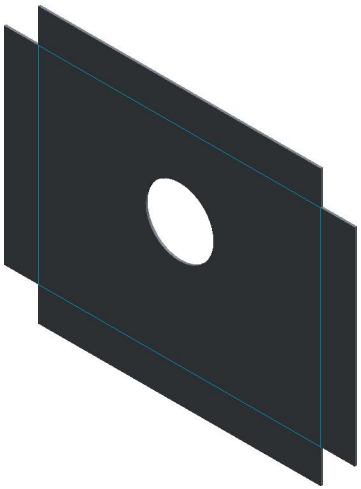

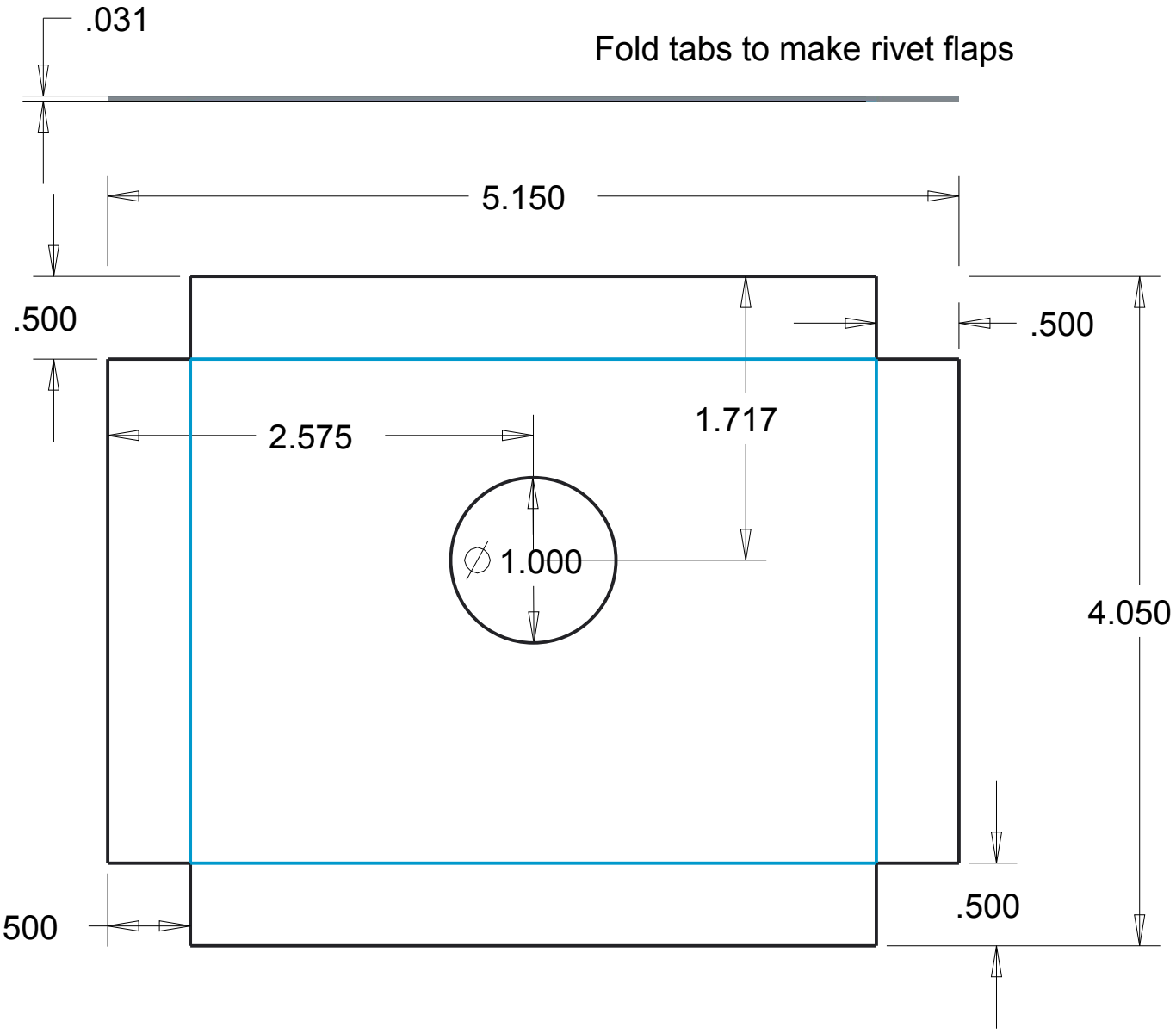

Ring Support

2 Required: 2024 Aluminum

All units in Inches

Scale 1:1 for all views

Note: Center hole must be drilled at a small angle from normal in order to line up with each other after being mounted on the side plates. This is acheived by drilling the holes while they are clamped to a plate with the same taper as the side support plates (see side plate drawing).